

TOPICAL REVIEW • OPEN ACCESS

Field-free approaches for deterministic spin-orbit torque switching of the perpendicular magnet

To cite this article: Hao Wu et al 2022 Mater. Futures 1 022201

View the article online for updates and enhancements.

You may also like

- Equilibria and precession in a uniaxial antiferromagnet driven by the spin Hall effect Qiao-Hua Li, Peng-Bin He, Meng-Qiu Cai
- Annealing effect on the magneto-electric properties of SOT-MTJs from micro to nano-sized dimensions
 Peiyue Yu, Lei Zhao, Jianfeng Gao et al.
- Critical switching current of a perpendicular magnetic tunnel junction owing to the interplay of spin-transfer torque and spin-orbit torque Do Hyung Kang, Ji-Hun Byun and Mincheol Shin

Mater. Futures 1 (2022) 022201 (13pp)

https://doi.org/10.1088/2752-5724/ac6577

Topical Review

Field-free approaches for deterministic spin-orbit torque switching of the perpendicular magnet

Hao Wu^{1,2,3,4,*}, Jing Zhang^{1,4}, Baoshan Cui¹, Seyed Armin Razavi², Xiaoyu Che², Quanjun Pan², Di Wu², Guoqiang Yu^{1,3,*}, Xiufeng Han^{1,3} and Kang L Wang^{2,*}

E-mail: wuhao1@sslab.org.cn, guoqiangyu@iphy.ac.cn and wang@ee.ucla.edu

Received 2 February 2022, revised 27 March 2022 Accepted for publication 6 April 2022 Published 22 April 2022



Abstract

All-electrical driven magnetization switching attracts much attention in next-generation spintronic memory and logic devices, particularly in magnetic random-access memory (MRAM) based on the spin—orbit torque (SOT), i.e. SOT-MRAM, due to its advantages of low power consumption, fast write/read speed, and improved endurance, etc. For conventional SOT-driven switching of the magnet with perpendicular magnetic anisotropy, an external assisted magnetic field is necessary to break the inversion symmetry of the magnet, which not only induces the additional power consumption but also makes the circuit more complicated. Over the last decade, significant effort has been devoted to field-free magnetization manipulation by using SOT. In this review, we introduce the basic concepts of SOT. After that, we mainly focus on several approaches to realize the field-free deterministic SOT switching of the perpendicular magnet. The mechanisms mainly include mirror symmetry breaking, chiral symmetry breaking, exchange bias, and interlayer exchange coupling. Furthermore, we show the recent progress in the study of SOT with unconventional origin and symmetry. The final section is devoted to the industrial-level approach for potential applications of field-free SOT switching in SOT-MRAM technology.

Keywords: spin-orbit torque, perpendicular magnetic anisotropy, field-free switching, symmetry breaking, magnetic memory

Original content from this work may be used under the terms of the Creative Commons Attribution 4.0 licence. Any further distribution of this work must maintain attribution to the author(s) and the title of the work, journal citation and DOI.

¹ Songshan Lake Materials Laboratory, Dongguan, Guangdong 523808, People's Republic of China

² Department of Electrical and Computer Engineering, and Department of Physics and Astronomy, University of California, Los Angeles, CA 90095, United States of America

³ Beijing National Laboratory for Condensed Matter Physics, Institute of Physics, Chinese Academy of Sciences, Beijing 100190, People's Republic of China

⁴ Co-first authors.

^{*} Authors to whom any correspondence should be addressed.

Future perspectives

Magnetic field-free approaches are important for next-generation spin—orbit torque driven magnetic random-access memory (SOT-MRAM) based on perpendicular magnetic anisotropy (PMA). The symmetry breaking is crucial to realize the deterministic field-free SOT switching, such as time reversal symmetry breaking by magnetic field, mirror symmetry breaking, chiral symmetry breaking and crystal symmetry breaking. These inspire exciting possibilities for field-free SOT switching by breaking more symmetries in the future: rotational symmetry breaking (magic angle), etc.

1. Introduction

In conventional electronics, only the charge degree of freedom of an electron is utilized to construct devices. The electron also possesses a spin angular momentum closely associated with the magnetic moment and is called spintronics [1]. The research field of spintronics exploits both charge and spin degrees of freedom of electrons to provide additional functionalities, such as non-volatility and reduced power consumption, compared to conventional electronic devices. Since 1988, scientists have discovered the giant magnetoresistance effect in multilayers [2, 3]. After that, the interaction between charge transport and electron spin in magnetic nanomaterials has become an essential factor in condensed matter physics. Its research not only laid the foundation for the emerging discipline of spintronics but also promoted the prosperity of materials science to a large extent and has shown an everincreasing application value and economic value, such as in hard-disk drive technology [4]. With the discovery of the tunnel magnetoresistance effect, magnetic tunnel junction (MTJ) has become more and more widely used in the spintronic industry [5-10]. Among them, the MTJ-based MRAM has become a research hotspot for its high endurance, low power dissipation, and high reading/writing speed.

In 1996, Slonczewski *et al* theoretically predicted the spin-transfer torque (STT) effect [11, 12]. The STT-MRAM designed and manufactured by the STT effect utilizes the electrical current to drive the magnetization switching, a new type of operation method of MRAM [13]. In recent years, researchers have proved that spin-orbit torque (SOT) can also be used to switch the magnetization direction. Compared to STT, SOT not only improves the switching speed but also separates the read and write channels, which effectively improves the endurance of the tunneling barrier for MTJ [14].

Although SOT is generated due to the accumulation of spins at the FM/NM interface, the detailed microscopic origin of the spin current generation is under debate and research. Two main spin—orbit coupling (SOC) phenomena are attributed to spin accumulation: bulk spin Hall effect (SHE) and interface Rashba-Edelstein effect. The SHE was theoretically predicted in 1971 by Dyakonov and Perel [15, 16], then revived by Hirsch in 1999 [17] and observed directly by using Kerr microscopy in 2004 [18]. The SHE exploits the bulk SOC in the NM layer to convert an unpolarized charge current into a pure spin current and can be represented by using

the equation: $J_{\rm S} = \frac{\hbar}{2e} \theta_{\rm SH} (J_{\rm C} \times \sigma)$, where $J_{\rm C}$ is the applied charge current, J_S is the spin current generated by the SHE, and σ is the polarization of the spin current. In addition, \hbar , e and $\theta_{\rm SH}$ denote the reduced Planck constant, elementary charge, and spin Hall angle (SHA), respectively. However, the Rashba-Edelstein effect (also called inverse spin galvanic effect [19]) mainly originates from an interfacial SOC phenomenon [20, 21] that arises in structures with broken inversion symmetry. Regardless of the potential origin of spin accumulation at the NM/FM interface, due to this non-equilibrium spin density, the SOT applied on the magnetization of adjacent FM can be decomposed into two components [22–24]: the damping-like (or Slonczewski) torque $\tau_{DL} \sim \mathbf{m} \times (\boldsymbol{\sigma} \times \mathbf{m})$ and the field-like torque $\tau_{\rm FL} \sim (\boldsymbol{\sigma} \times \mathbf{m})$, where \mathbf{m} and $\boldsymbol{\sigma}$ represent the directions of the magnetization and the spin polarization, respectively. SOT-driven magnetization switching is a bipolar-type switching, where the current polarity needs to be reversed for the back-and-forth switch of up and down magnetizations, different with the polar behavior in the magnetization switching process induced by the optical or thermal pulses. At present, the MTJ device with PMA is designed as the unit cell SOT-MRAM due to its high thermal stability. However, for the perpendicular magnet, it is generally necessary to apply a magnetic field in a specific direction to break the symmetry and determine the perpendicular direction of the magnet due to the in-plane effective field (both damping-like and field-like) from SOT [25-29]. The requirement for the assistant field is a major obstacle for the application of SOT in the industry. Therefore, magnetic field-free SOT switching has become one of the key bottlenecks for the realization of SOT-MRAM [30]. In this review, based on the symmetry analysis, we mainly focus on several field-free approaches for deterministic SOT switching, such as lateral structural symmetry breaking, chiral symmetry breaking, exchange bias and interlayer exchange coupling, SOT with unconventional origins/symmetry, and the industrial approach for applications.

2. Lateral structural symmetry breaking

Field-free deterministic SOT switching with lateral structural symmetry breaking relies on the introduction of a currentinduced out-of-plane effective magnetic field. The direction of this new field $(+\hat{z} \text{ or } -\hat{z})$ is determined by the current polarity. Consequently, it breaks the symmetry between up/down magnetization states and facilitates field-free switching. In conventional heterostructures, the inversion symmetry is only broken along the stack deposition direction (z axis). However, with lateral structural asymmetry, symmetry is also broken with respect to the x-z plane, and the only existing mirror symmetry is along the x axis (current direction), as shown in figures 1(a) and (b). Consequently, current-induced effective SOT fields should be transformed as pseudo-vectors only under reflections in the y-z plane, which allows for the introduction of perpendicular effective fields $H_z^{\rm FL}$. Reversing the current direction in this case results in the reversal of $H_7^{\rm FL}$ direction [31].

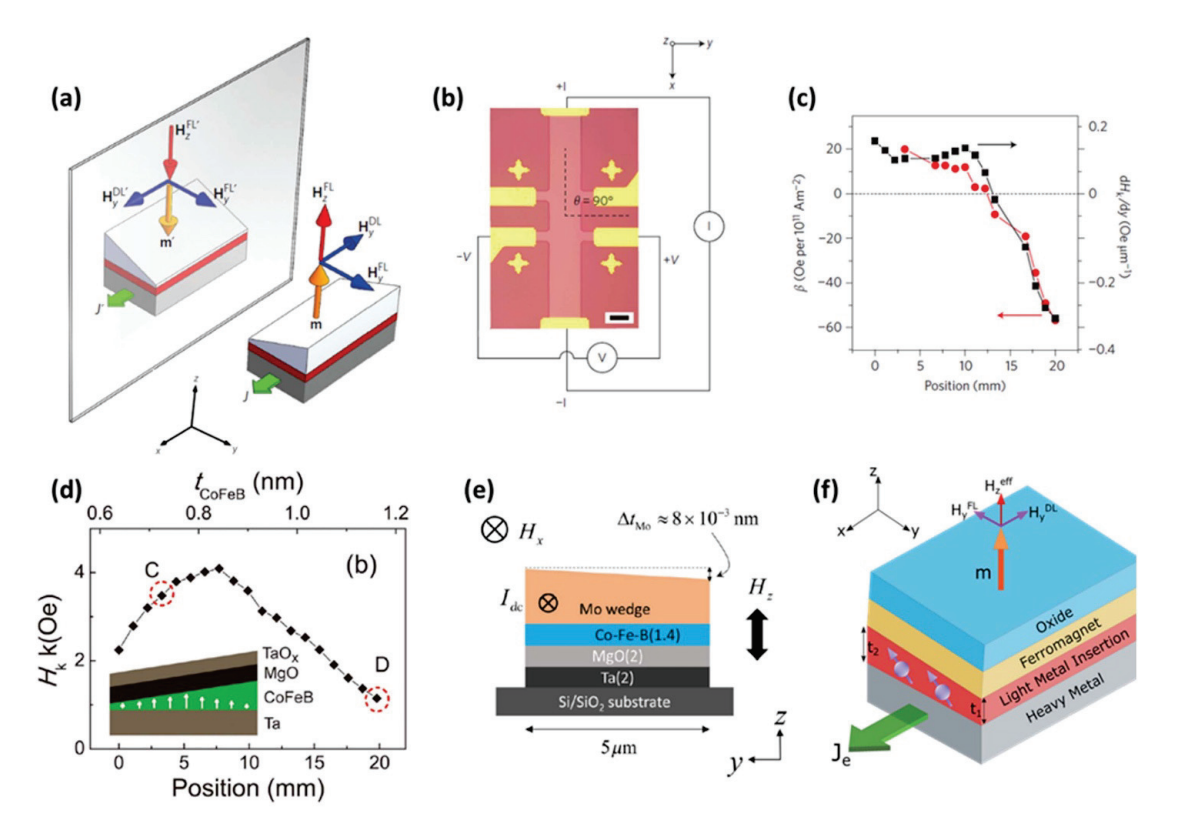


Figure 1. Lateral structural symmetry breaking for field-free deterministic SOT switching. (a) Broken mirror symmetry in the lateral direction allows for the creation of effective perpendicular magnetic fields H_z^{FL} [31]. (b) Measurement configuration: current is applied along the x direction, and structural symmetry is broken along the y direction, i.e. current and wedge directions are perpendicular to one another [31]. (c) Close correlation observed between H_z^{FL} and the magnetic anisotropy gradient dH_k/dy . (a)–(c) Reproduced from [31], with permission from Springer Nature. (d) Similar results are obtained using a wedge-shaped ferromagnet, CoFeB in this case. A correlation between the anisotropy gradient and H_z^{FL} is also found in this work. Reprinted from [32], with the permission of AIP Publishing. (e) Current-induced effective perpendicular magnetic fields created using a wedge-shaped SOC layer Mo. Reprinted figure with permission from [33], Copyright (2018) by the American Physical Society. (f) Creation of effective perpendicular fields using a thin asymmetric light-metal insertion. Reprinted with permission from [34]. Copyright (2020) American Chemical Society.

In experiments, introducing a wedge-shaped layer in the heavy-metal/ferromagnet/oxide heterostructure yields an effective structural symmetry breaking. In the earliest experimental work in this regard, a wedge-shaped oxide was deposited by oblique angle sputtering without substrate rotation [31]. A linear correlation was found between $H_z^{\rm FL}$ and the applied current density, with the slope defined as $\beta = \frac{\partial H_{\epsilon}^{\rm FL}}{\partial J}$. The authors also found a very strong correlation between β and the PMA gradient along the wedge direction $\frac{\partial H_k}{\partial y}$, with H_k defined as the effective anisotropy field (figure 1(c)). Later on it was shown that similar results could be obtained by using a wedge-shaped ferromagnet [32], SOC layer [33, 35, 36], and even a thin wedge insertion layer [34, 37, 38], as shown in figures 1(d)–(f). H_z^{FL} generically appears in all these works, although their material systems are widely different, which points to the important role of symmetry breaking. In addition to $H_z^{\rm FL}$, the conventional SOT effective damping-like $(H_x^{\rm DL})$ and field-like $(H_v^{\rm FL})$ fields are also present in such heterostructures. The competing effect of all these fields in the switching process has also been studied. It has been shown that at zero external field, the switching process is driven by H_z^{FL} ; and for large external fields, switching is determined by the conventional SOTs, especially H_x^{DL} [39].

Several mechanisms have been proposed to explain the microscopic creation of H_z^{FL} and the field-free switching process. (a) Interfacial Rashba-Edelstein effect [31, 34]: by breaking the inversion symmetry along the lateral direction, microscopic effective electric fields are allowed along the y axis. According to the Rashba SOC Hamiltonian $H_R = \frac{\alpha_R}{\hbar} \sigma_p$. $(E \times p)$ [19, 21], out-of-plane effective magnetic fields are then expected upon the application of a charge current along the x axis. Here, α_R , \hbar , σ_p , E, and p are the Rashba parameter, reduced Planck constant, Pauli matrices, effective electric field, and electron momentum, respectively. (b) Tilting of the poly-crystalline structure or anisotropy axis because of oblique angle deposition of the wedge layer [33, 40, 41]: a possible tilt of the crystal structure can lower down the structure's symmetry and allow for the creation of perpendicular effective fields, similar to the effect observed in WTe₂ [50]. Alternatively, if the magnetic anisotropy axis is tilted away

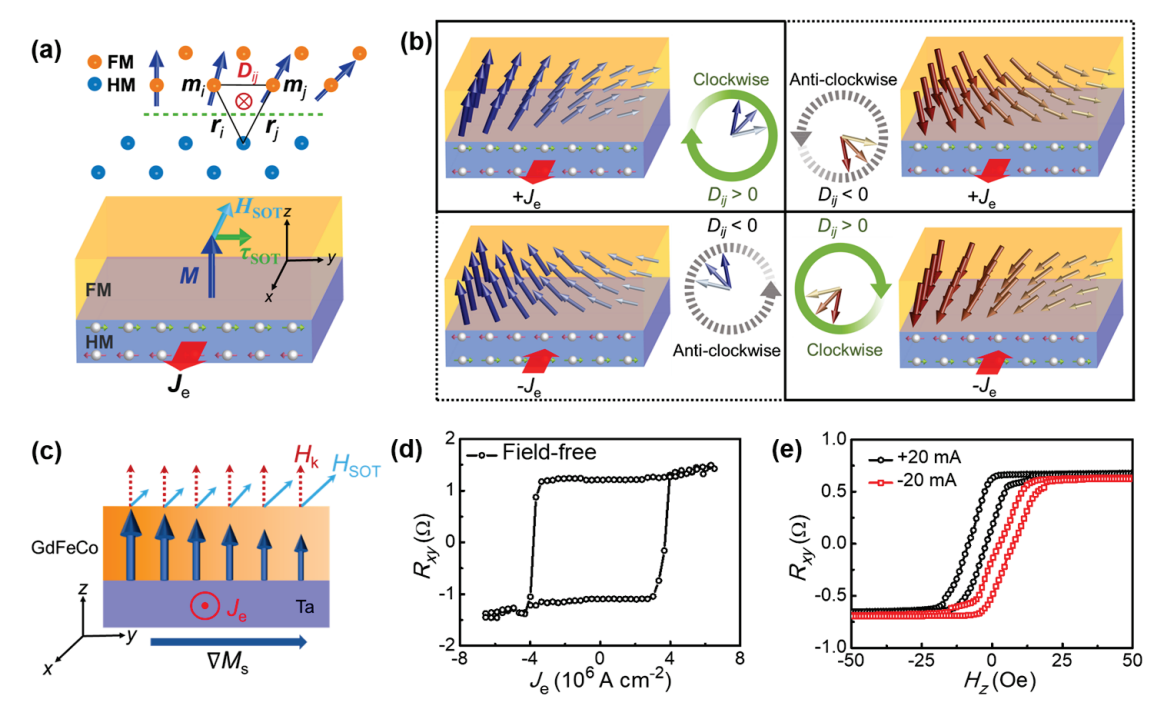


Figure 2. Chiral symmetry breaking determined SOT switching for the lateral magnetization gradient. (a) DMI and SOT in the heavy/metal/ferromagnet system. (b) For the lateral magnetization gradient, the SOT exerts the non-collinear spin textures, where the chirality of the spin textures is performed by the DMI, leading to the deterministic switching. (c) The composition gradient of GdFeCo can generate a saturation magnetization gradient along the y direction ($\nabla_y M_s$). (d) Chiral symmetry breaking determined field-free SOT switching in Ta/GdFeCo structures with a $\nabla_y M_s$. (e) Under ± 20 mA currents, the anomalous Hall loops are shifted to the opposite directions, indicating the z-component effective field H_z^{eff} from chiral symmetry breaking. Reprinted with permission from [49]. Copyright (2021) American Chemical Society.

from the z axis, the symmetry between up/down magnetization states is effectively broken and field-free SOT switching could be realized by the conventional damping-like SOT scenario, due to the in-plane component of M. A tilt in the anisotropy axis could be realized using the sputtering process [40], or by partially covering the ferromagnet with an oxide layer [42].

From the applications point of view, using an in-plane structural asymmetry is supposed to be not desirable for waferscale fabrication if an inhomogeneity of the magnetic properties exists in the film. However, it has been shown that by using an asymmetric light-metal insertion, the magnetic anisotropy, coercivity, SOTs, switching current density could all be almost uniform across the whole sample, where the key is the low SOC of light metals [34]. Furthermore, the scalability of using wedge samples for field-free switching has also been studied, where the same β values are obtained even if the device dimensions are shrunk by two orders of magnitude [34]. One of the interesting questions that still need to be addressed is the relationship between the β values and the slope of the wedge layer. This is potentially important for further reduction of the wedge layer's thickness difference across the wafers and paving the way for the practical application of this strategy for field-free switching.

3. Chiral symmetry breaking

Besides mirror symmetry, chiral symmetry is very important in magnetic systems. The chiral symmetry could be broken by the non-collinear Dzyaloshinskii–Moriya interaction (DMI) [43–46], which leads to the chiral spin textures such as the Néel-type domain walls and skyrmions [47, 48]. The Hamiltonian of DMI can be written as $\hat{H}_{\rm DMI} = \sum_i -D_{ij} \cdot (m_i \times m_j)$,

where D_{ij} is the DMI tensor between m_i and m_j . For a magnetic system with a gradient of magnetic properties, such as in-plane saturation magnetization (M_s) gradient in ferrimagnetic GdFeCo, which can be realized by a composition gradient due to the antiferromagnetically-coupled Gd and CoFe lattices, when we apply a current, the SOT will exert a spin texture because of $H_{SOT} = \frac{\hbar \theta_{SH}J_c}{2|e|M_st}$, where \hbar is the reduced Planck constant, t is the thickness of the magnetic layer, and e is the elementary charge. Figure 2(b) shows the four possible configurations between the current and the spin textures, for a given DMI, such positive DMI in Ta/GdFeCo system prefers the right-hand chirality due to the lower DMI energy, and thus select the $+M_z$ and $-M_z$ magnetizations for $+J_c$ and $-J_c$, respectively, i.e. deterministic SOT switching is achieved [49].

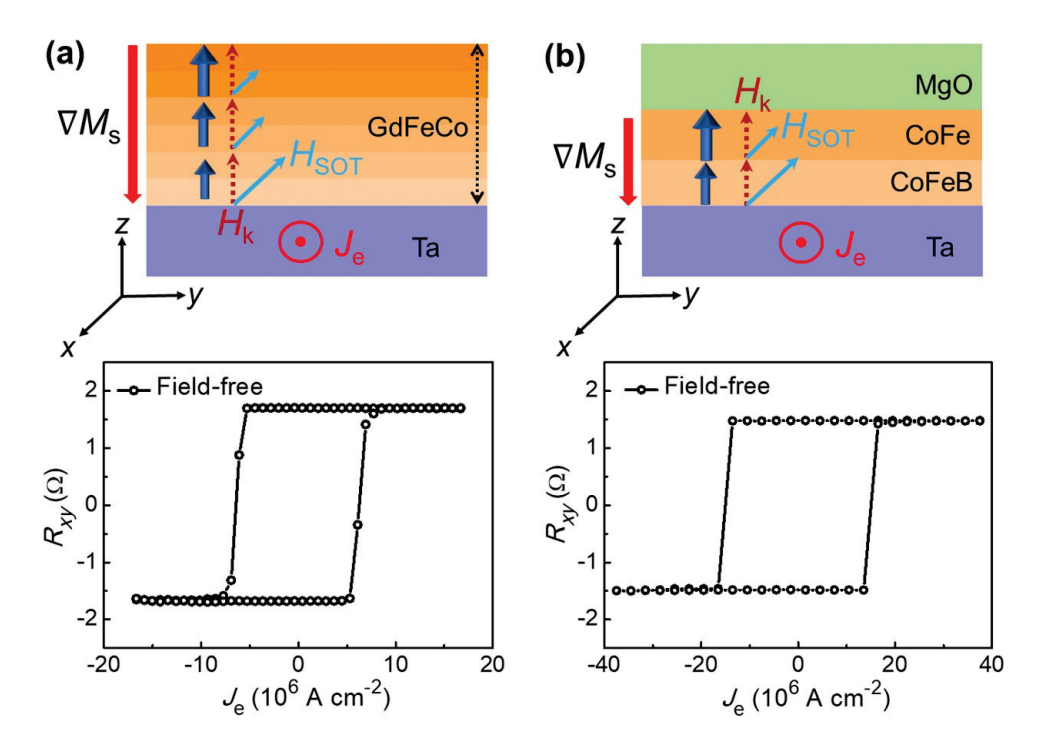


Figure 3. (a) For the vertical magnetization gradient in Ta/GdFeCo, the chiral symmetry of the SOT-induced spin textures along the thickness direction can be broken by the DMI, and thus contributes to the deterministic switching. (b) Even for the CoFeB/CoFe bilayer structure with a small M_s gradient, the chiral symmetry breaking determined SOT switching is still robust. Reprinted with permission from [49]. Copyright (2021) American Chemical Society.

In order to form the saturation magnetization gradient $\nabla_y M_s$, we co-sputter the Gd and FeCo in the opposite direction by the same speed so that a composition gradient is formed while the thickness is still uniform, as shown in figure 2(c). In this way, the non-collinear spin textures are formed during the gradient SOT strength, and thus the interfacial DMI breaks the chiral symmetry and then determines the field-free SOT switching, as shown in figure 2(d). The SOT-induced anomalous Hall loop shift results are shown in figure 2(e), and the R_{xy} – H_z curves are shifted to the opposite directions for ± 20 mA currents, indicating an out-of-plane effective field by a combination of chiral symmetry breaking and SOT, which supports the field-free SOT switching.

However, the lateral magnetic gradient leads to the varied device performance in the wafer scale, and thus makes it not practical for industry-level applications. Therefore, we design the vertical magnetic gradient in Ta/GdFeCo and Ta/CoFeB/CoFe/MgO with an increasing M_s , as shown in figures 3(a) and (b). In this case, the DMI determines the chirality of the SOT-induced spin textures along the thickness direction, and thus contributes to the deterministic SOT switching. It is worth noticing that the conventional interfacial DMI contribution is zero for the vertical spin textures, and the interlayer DMI plays the important role in this case, which has been discovered recently by the chiral interlayer exchange coupling phenomenon in multilayer systems [51–56].

4. Field-free switching by exchange-bias and interlayer exchange coupling

One approach to realize deterministic magnetization switching without the assistance of an in-plane external magnetic field is harnessing the exchange-coupling effect on an FM layer in the in-plane direction that can break the mirror symmetry. Such in-plane exchange-coupling can be achieved by interfacing the FM layer with an AFM layer, where an exchange bias will be established on the FM layer. Fukami et al demonstrated that in a Co/Ni/PtMn multilayer system, after field annealing in the x-direction, the exchange bias from the AFM PtMn layer can tilt the perpendicularly magnetized Co/Ni layers adjacent to the PtMn layer towards the in-plane direction, as illustrated in figure 4(a) [57]. The exchange bias can be observed from the magnetic hysteresis loop in the x-direction by SQUID measurements as shown in figure 4(b). Meanwhile, the SOC from PtMn (SHA $\sim+0.1$.) can exert SOT that is sufficiently large to switch the magnetization in the Co/Ni layer after applying current pulses. Due to the in-plane exchangebias that breaks mirror symmetry, magnetization switching at zero field is observed, and the switching loop vanishes when the exchange-bias is compensated by an external field of -10 mT (figure 4(c)). Additionally, by applying current pulses with different amplitudes, the portion of the reversed magnetization can be controlled to exhibit a memristor-like

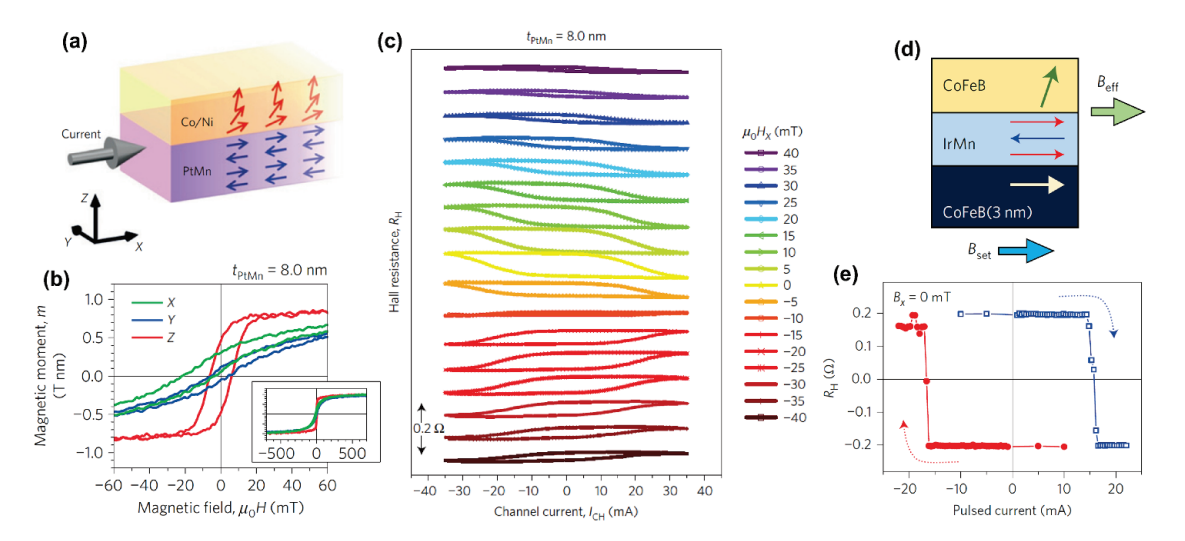


Figure 4. Exchange-bias and field-free magnetization switching in FM/AFM structures. (a) Schematic illustration of an exchange-biased system comprised of Co/Ni and PtMn. While the Co/Ni layer shows PMA, the magnetization is canted by the exchange coupling from the AFM PtMn layer that breaks mirror symmetry [57]. (b) Magnetic hysteresis loops of the Co/Ni/PtMn structure along *x*, *y* and *z* directions after field annealing in *x*-direction [57]. An in-plane exchange-bias is established as indicated by the green curve (c) SOT switching of the Co/Ni/PtMn structure under different external magnetic fields and at zero field. (a)—(c) Reproduced from [57], with permission from Springer Nature. (d) Schematic illustration of a CoFeB/IrMn/CoFeB system. (e) Field-free SOT switching of the CoFeB/IrMn/CoFeB structure after field annealing. (d), (e) Reproduced from [58], with permission from Springer Nature.

switching behavior. Field-free magnetization in the FM/AFM exchange-biased system is also demonstrated by Oh *et al* and Zhao *et al* in CoFeB/IrMn structures. However, magnetization switching loops with incomplete switching are observed [58–61]. The partial magnetization switching is not desirable and can result in critical issues in the application. Oh *et al* pointed out that a weak exchange bias from the AFM IrMn layer could be responsible for the incomplete magnetization switching. To enhance the exchange-coupling, an additional CoFeB layer is introduced beneath the IrMn layer, which contributes to field-free switching with complete switching loops (figures 4(d) and (e)).

The phenomenon of partial switching at zero field in FM/AFM structures is also observed by van den Brink et al in a IrMn-based structure (figure 5(a)) [62]. Differ from the weak exchange-bias argument by Oh et al, another model is proposed to account for the physical origin of such effect. In the proposed model, the polycrystalline morphology nature of the sputtered IrMn is taken into consideration, and the incomplete switching is attributed to the antiferromagnetic grains with different local exchange-bias directions in the IrMn layer. While the homogenous external field can reorient the perpendicular magnetization in the same direction to achieve complete switching, the local exchange-bias shown in figure 5(b) is inhomogeneous after field annealing, causing opposite switching directions in local grains if the current is not perfectly along the exchange-bias direction. Besides the multi-grain effect, our previous investigation suggests that the Joule heating effect can also impact the switching ratio at zero field in a FM/AFM system. Figure 5(c) shows a schematic of the Pt/CoFe/IrMn structure used in the field-free switching study, where the IrMn layer offers exchange-bias and the Pt layer contributes to the SOT via SHE. After multiple switching loops, it is observed that the switching ratio drops by more than 70% as displayed in figure 5(d). The decreasing portion of the reversed magnetization after multiple switching loops can be attributed to the Joule heating effect, which raises the system temperature during each switching loop and results in a decreasing in-plane exchange-bias as well as a reduced switching ratio (figure 5(d)) [63].

Apart from adopting an adjacent AFM layer to induce exchange-bias on the FM layer, another viable approach to break mirror symmetry is utilizing the interlayer exchangecoupling between two FM layers with a spacing layer. Lau et al demonstrated a Pt/CoFe/Ru/CoFe/IrMn structure where the two CoFe layers with different thicknesses are exchange-coupled with each other with a Ru spacer in between (figure 6(a)) [64]. The bottom CoFe layer with lower thickness (0.7 nm) manifests PMA and serves as the free layer. The top CoFe layer with higher thickness (2 nm) is the fixed layer, which possesses in-plane magnetic anisotropy and is exchange-biased by the AFM IrMn layer that pins the magnetization in the in-plane direction. The interlayer exchangecoupling between the two CoFe layers cants the perpendicular magnetization of the bottom CoFe layer toward the in-plane direction similar to the effect of an external magnetic field. As a result, the magnetic hysteresis loop in the x-direction is shifted as displayed in figure 6(b). In such a way, the mirror symmetry of the perpendicular magnetization is broken and field-free switching is demonstrated (figure 6(c)). Meanwhile, the interlayer exchange-coupling is still sufficiently strong to assists field-free switching after replacing the Ru spacer with Pt or slightly modifying the spacer thickness. Murray et al pointed out that the interlayer exchange-coupling can still be achieved without an AFM layer [65]. Figure 6(d) schematically shows the CoFeB/W/CoFeB structure with the CoFeB

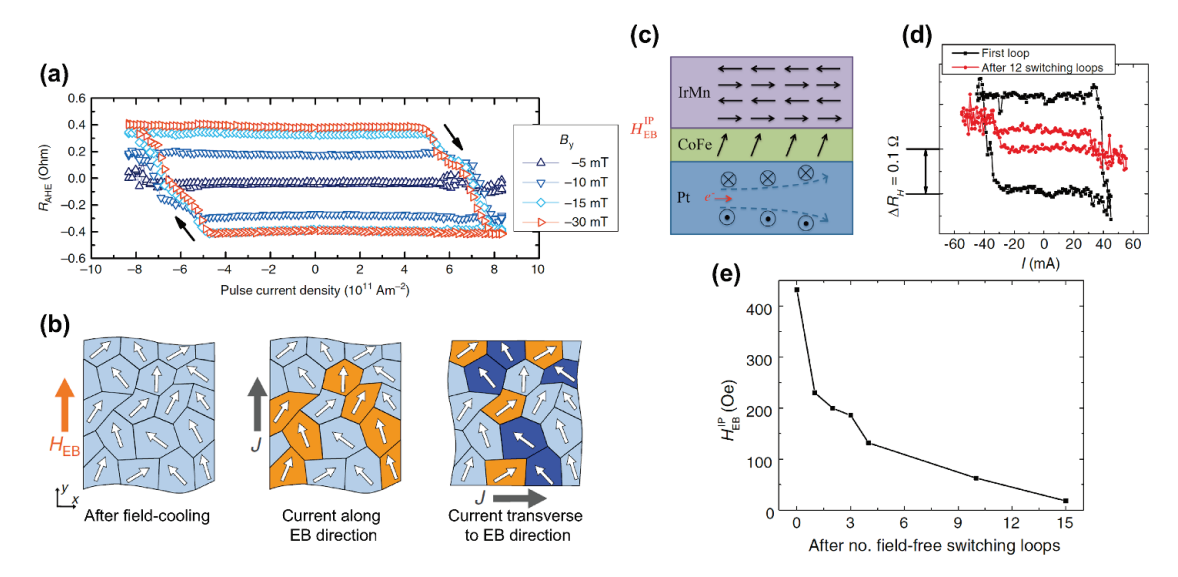


Figure 5. Partial switching and Joule heating effect in IrMn-based FM/AFM structures. (a) Magnetization switching loops of a Pt/Co/IrMn structure under different in-plane external magnetic fields. The magnetization switching is not complete at zero field [62]. (b) Sketches of grains within the antiferromagnetic layer after field annealing. (a), (b) Reproduced from [62]. CC BY 4.0. (c) Schematic illustration of a Pt/CoFe/IrMn structure [63]. (d) Comparison of the SOT switching loops between the first switching test and after multiple SOT switching loops. The anomalous Hall resistance change after switching significantly decreases from \sim 0.2 Ω to \sim 0.05 Ω after 12 SOT switching loops [63]. (e) Decreasing in-plane exchange-bias after multiple SOT switching loops. (c)–(e) Reprinted figure with permission from [63], Copyright (2017) by the American Physical Society.

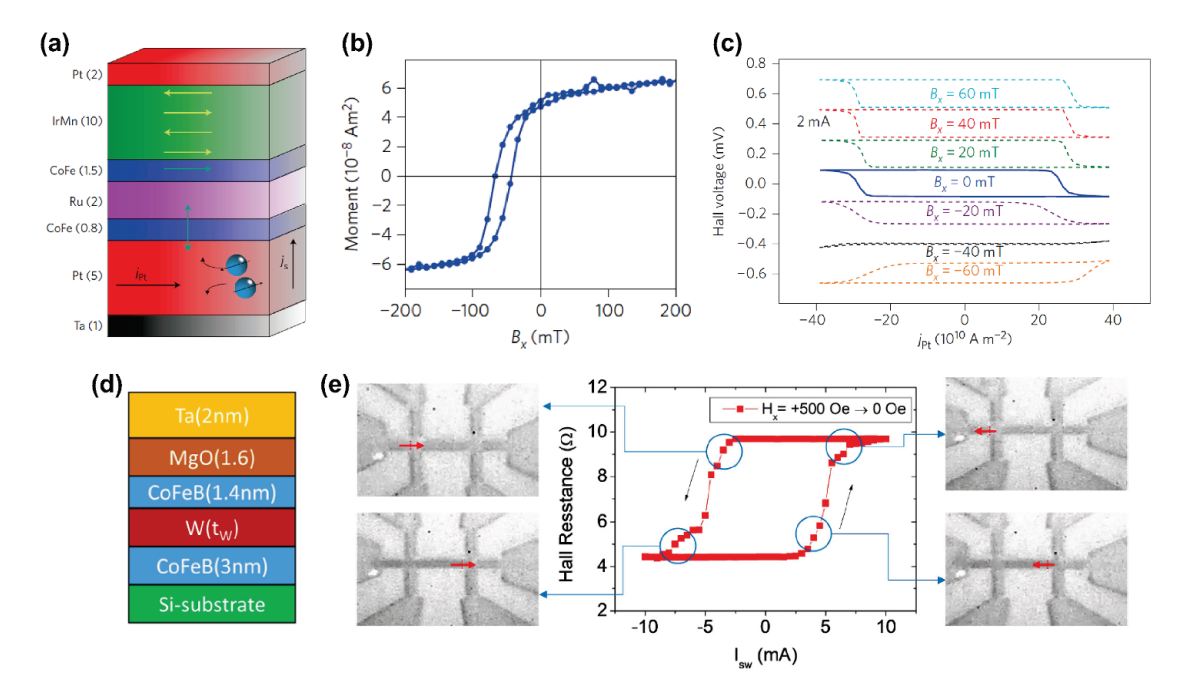


Figure 6. Field-free magnetization switching through interlayer exchange-coupling. (a) Exchange-coupled CoFe layers with a Ru spacer. The top CoFe layer with in-plane magnetic anisotropy exchange-biased by IrMn serves as the fixed layer and couples with the bottom CoFe layer with PMA. SOT originates from the Pt layer via SHE [64]. (b) Shifted magnetic hysteresis loop in the *x*-direction as a result of the interlayer exchange-coupling [64]. (c) SOT switching under different external magnetic fields and at zero field. (a)–(c) Reproduced from [64], with permission from Springer Nature. (d) CoFeB/W/CoFeB structure with the two CoFeB layers coupled with each other. The W spacer here also contributes to SOT in this system [65]. (e) Field-free SOT switching investigated by both transport and MOKE measurements. (d), (e) Reprinted figure with permission from [65], Copyright (2019) by the American Physical Society.

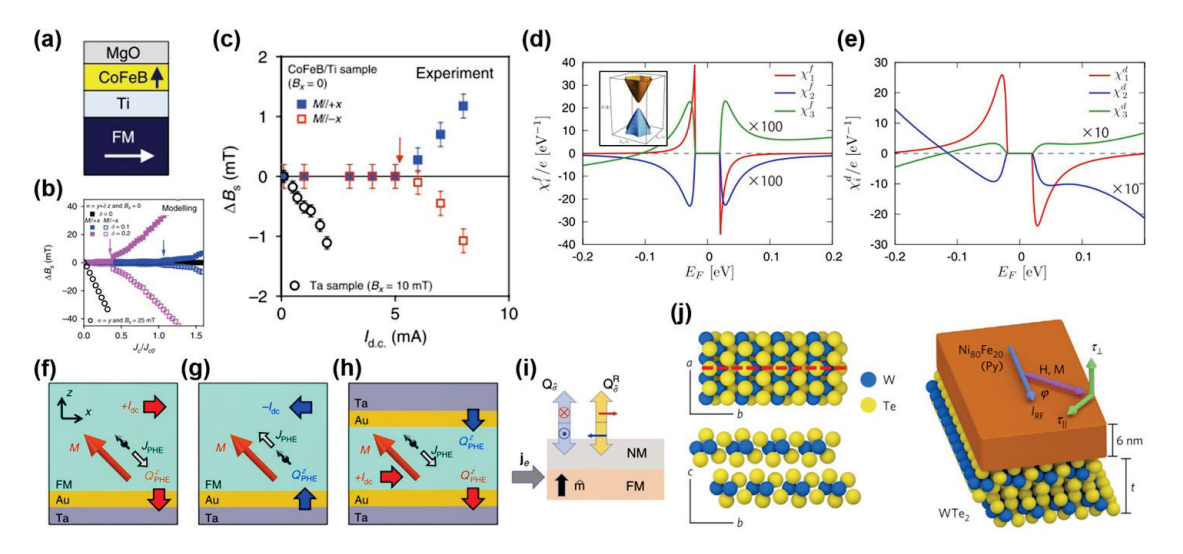


Figure 7. Emerging studies in SOTs with unconventional symmetry. (a) Schematic of the HM/FM-based structures for generating spin currents with OOP components [87]. (b), (c) Experimental results shown in (c) qualitatively agree with micromagnetic simulation results for the cases of spin currents with non-zero OOP spin components $\delta \neq 0$, labelled by purple and blue squares in (b) these non-zero OOP spin components facilitate field-free SOT switching. (a)–(c) Reproduced from [87], with permission from Springer Nature. (d), (e) The analytical estimation of coefficients χ (which parameterize spin density induced by an electric field) in a magnetic TI for (d) field-like spin torques and (e) damping-like spin torques. Inset in (d) depicts the band structure of a magnetic TI when high-order momentum contributions are involved at energy level away from the Dirac point. (d), (e) Reprinted figure with permission from [88], Copyright (2019) by the American Physical Society. (f)–(h) Schematics of the pure spin current generated by the planar Hall effect. Reproduced from [89], with permission from Springer Nature. (i) Schematics of SOTs with spin rotation symmetry (labelled by $\mathbf{Q}_{\hat{\sigma}}^{R}$) in comparison with those with conventional symmetry (labelled by $\mathbf{Q}_{\hat{\sigma}}^{R}$). Reproduced from [90]. CC BY 4.0. (j) Schematic of the bilayer WTe₂/Permalloy structures where field-free switching is realized due to the reduced symmetry of the WTe₂ surface. Reproduced from [50], with permission from Springer Nature.

layers spaced by the W layer, which generates SOT on the top CoFeB layer at the same time. While field-free switching is also realized in this system, it is reported that the observed switching by Kerr imaging primarily originates from domain nucleation and domain wall motion (figure 6(e)). On the other hand, micromagnetic simulation indicates that the roughness-caused Néel coupling could be a more critical effect in achieving the field-free deterministic switching than stray field contribution. The above phenomena might pose an obstacle in using this material structure for memory application.

5. Spin-orbit torque with unconventional origins and symmetry

Undoubtedly, the necessary symmetry breaking to realize deterministic SOT-switching of perpendicular magnetization is essentially associated with the symmetry of SOT itself [66]. Correspondingly, the emerging studies on SOTs with unconventional origins and the vectorial dependence of SOTs on magnetic orders beyond the lowest order approximation not only provide insights into the symmetry of SOTs but also lead to new opportunities in developing novel field-free switching schemes [67, 68]. In this section, we review some of the pioneering observations of SOTs with atypical origins and symmetry.

The transverse voltage occurs in a magnetic material when an electric field is present, the so-call anomalous Hall effect, originates in the imbalance of electrons with opposite spins, and therefore, indicates that along with the accumulation of charge at the opposite sides of the material, a non-equilibrium spin accumulation will also occur. Like the spin accumulation induced by SHE in a single heavy metal layer, such a spin accumulation produced by magnetic materials can also be harvested and produce sizeable SOTs. This can be viewed as an magnetic contribution to the chargeto-spin conversion/SHE [69]. This type of contribution to SOTs has been experimentally demonstrated in common ferromagnets [70–74, 87], ferrimagnets [75], and antiferromagnets [76] with efficiency comparable to heavy metals and showed unusual behaviors (as shown in figures 7(a)-(c)). Moreover, antiferromagnets potentially allow the non-trivial control of SOTs through either collinear or non-collinear magnetic structures [69, 76, 77]. Recently, the magnetic spin Hall effect in non-collinear antiferromagnets have been reported to provide the out-of-plane spins, either by the cluster magnetic octupole or the momentum-dependent spin splitting, shedding light on the new directions for the field-free SOT switching [78, 79].

Theoretical calculation also suggests the SOTs from AHE can be effectively controlled by electric fields applied to ferromagnets or reducing symmetry in ferromagnets [80]; Compared with SOTs with common symmetry which requires

the directions of spin polarization, spin-current flow and charge-current flow are mutually orthogonal (i.e. in common HM/FM heterostructures, a charge-current flow in x direction will generate spin flowing toward z direction into FM layer with a polarization pointing along y direction), the incorporation of magnetic orders allows generating a spin accumulation deviating from y direction for SOTs and field free-switching enabled by this additional spin accumulation has been demonstrated in pioneering experimental works [81, 82].

Beyond using magnetic orders to generate nonconventional SOTs, the SOTs generated by topological insulators (TIs) have spin polarization that are significantly depend on azimuthal angle of the magnetization, i.e. the direction of in-plane ferromagnetic orders [83]. An anisotropic antidamping-like SOT unique to TIs was identified in addition to the conventional SOTs and was found to be originated in a diffusive motion of conduction electrons [84]. Compared to ferromagnets, different behaviors of nonequilibrium (staggered) spin density and SOTs were found in a TI/antiferromagnet heterostructure where Dirac cone is preserved [85]. By including the higher order contributions of momentum k^2 terms and the hexagonal warping, studies in figures 7(d) and (e) theoretically predicted four new types of the SOT in addition to the conventional field-like and the damping-like torques while experimental demonstration is still unexplored [88].

Garello et al [66] provides a comprehensive summary on the symmetry of SOTs from conventional sources (SHE and Rashba effect), wherein the (higher-order) anisotropic (angledependent) torques and contributions from planar Hall effect were usually neglected. This study was experimentally completed by [86] recently, while the later prediction on planar Hall effect was confirmed in [89] (as shown in figures 7(f)–(h)) where researchers showed a spin-polarized electric current related to anisotropic magnetoresistance and the planar Hall effect can additionally generate large damping-like SOTs with an unusual angular symmetry. It has also been demonstrated the conventional SOTs near the magnetic interfaces exhibit a very different symmetry, namely spin-rotation symmetry (as shown in figure 7(i)), where the spin polarization is rotating about the magnetization [90]. Furthermore, to achieve better control of SOTs, the intrinsic symmetries can be modified and free-field switching can be achieved by utilizing spinsource materials with reduced crystal symmetries [41, 50, 91] (as shown in figure 7(j)); magneto-crystalline anisotropy design [92, 93], modulating the interfacial chemistry with electric fields [94].

Actually, in addition to the material design, it is crucial to combine SOT with the VCMA (the voltage-controlled magnetic anisotropy) effect to accomplish the switching in SOT-MRAM with lower critical switching current I_{SOT}. VCMA can change the interfacial magnetic anisotropy with a voltage across the barrier in MTJs and he voltage pulse can reflect the change between two stable magnetization states with reduced power dissipation and enhanced scalability. Recently, the VCMA effect has been introduced in the p-MTJ with the AFM/FM/Oxide structure to modulate the critical I_{SOT} [95].

6. Industrial approach for applications

Due to the high density, nonvolatility and fast writing speed, SOT-MRAM has wide potential application. In order to take full advantage, it is critical to break the inversion symmetry by a manufacturable approach to achieve the field-free switching for practical application.

Several manufacturable methods to break the symmetry are developed recently. One of the approaches is utilizing a build-in in-plane stray field [64, 96]. A 50 nm Co hard mask layer provides an in-plane bias magnetic field exerting on the free layer [96] shown in figure 8(a). Due to the small distance (~80 nm) between Co and free layer, the stray field can be as large as 36 mT, which is sufficient to most SOT devices for symmetry breaking. However, this method is not suitable for the high-density device integration. Sub-ns writing and high endurance performance is achieved as shown in figure 8(b). Besides, it should be noted that Co is considered as an alternative conductors for back end of line (BEOL) especially for beyond 7 nm process [97], which makes this method suitable for advanced technology node.

Secondly, inversion symmetry can be broken by canted MTJ devices, shown in figure 8(c). The MTJ is patterned to elliptical pillar, and the major axis of ellipse cants an angle to heavy metal line. Zhaohao *et al* simulated the field-free SOT switching in elliptical MTJs [98–100]. Because the component of the uniaxial shape anisotropy field along with the current channel breaks the inversion symmetry, field-free switching is achieved on those elliptical MTJ devices. Honjo *et al* first demonstrated the field-free switching based on canted SOT-MTJs, under 300 mm BEOL process full compatible with 400 °C thermal tolerance [101]. They achieved fast write speed of 0.35 ns without an external magnetic field shown in figure 8(d).

It is well known that STT effect breaks the inversion symmetry intrinsically. Therefore, three-terminal devices combining STT and SOT effect may be a promising approach to achieve the field-free switching [14, 102]. In this case, the STT current density is 10% of the threshold current of switching by STT solely, and STT current does not dominate the switching behavior. Even though the STT current passing through MTJ devices is small, the inversion symmetry can be broken by STT. Hence, SOT-induced field-free magnetization switching takes place. The approach is not compromising the original sub-ns writing and endurance.

In addition to above approaches, field-free SOT switching also may be achieved by other methods. Utilizing the inplane exchange bias effect [57] induced by antiferromagnetic layer adjacent to free layer to break the symmetry may be an optional method as well. However, the energy consumption may be an issue due to the small SHA of IrMn/PtMn comparing with Ta or W. On other hand, field-free switching is also achieved based on the type-y geometry of SOT [103, 104], strain effect [105] and wedged samples [31]. However, those approaches may be compromising on the device density, fabrication compatibility and energy consumption.

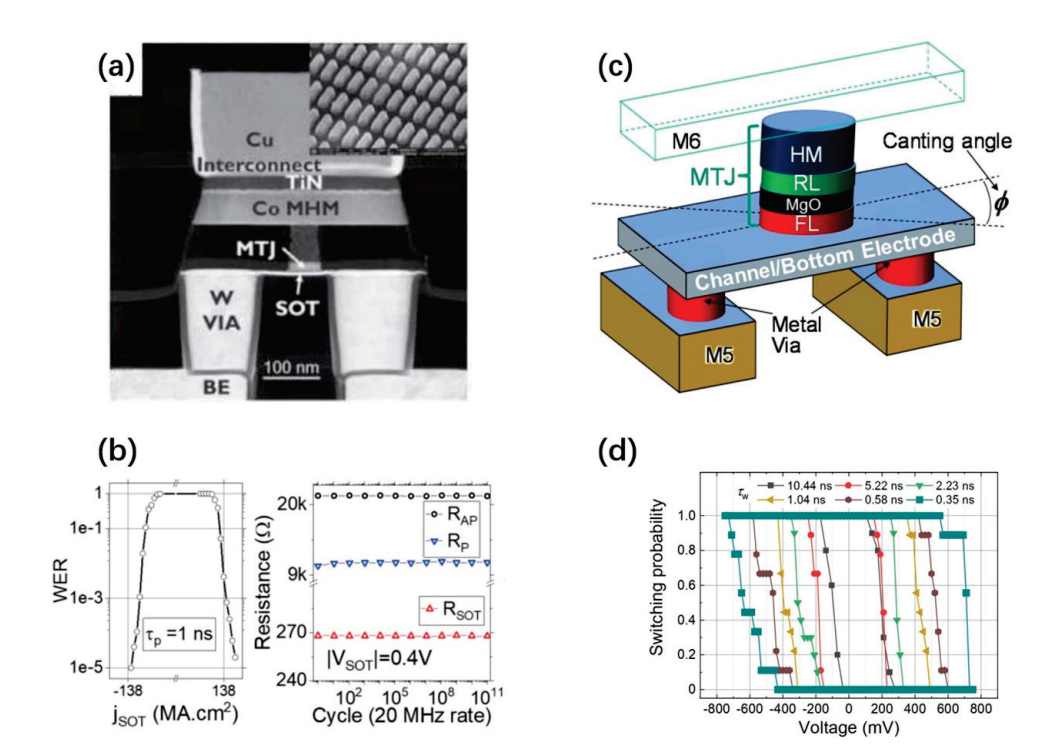


Figure 8. (a) Lateral cross-section transmission electron microscope (TEM) view of the SOT-MRAM cell with 50 nm thick Co magnetic hard mask (inset is the top view after etching) [96]. (b) Writing error rate and endurance measured on 60 nm MTJ devices with Co hard mask. (a), (b) © [2019] IEEE. Reprinted, with permission, from [96]. (c) Sketch of canted SOT-MRAM cell structure [101]. (d) Switching probability at different write pulse width for canted MTJ. (c), (d) © [2019] IEEE. Reprinted, with permission, from [101].

7. Conclusion and outlook

The seminal observation of field-free SOT switching in 2014 kicked off an intense research effort that has rapidly led to advances both in the understanding of the underlying physical mechanisms and in the realization of SOT-hosting systems suitable for application. It is now possible to achieve field-free SOT switching by several schemes, but some pending questions still need to be addressed. For example, field-free SOT switching is driven by the current-induced out-of-plane effective magnetic field, however, the microscopic and quantitative understanding of SOT-induced out-of-plane effective field is still incomplete. Furthermore, exploring the field-free SOT switching in quantum materials such as TIs/semimetals and two-dimensional materials will be a crucial step for reducing the power consumption for future SOT-MRAM. Besides those, novel device applications based on field-free SOT switching will be an important direction in the future, such as logic-inmemory computing and neuromorphic computing.

Acknowledgments

This work was supported by start-up funding support from Songshan Lake Materials Laboratory (Y1D1071S511), NSF Award Nos. 1935362, 1909416, 1810163 and 1611570, the U.S. Army Research Office MURI program under Grant Nos. W911NF-16-1-0472 and WN911NF-20-2-0166, and the National Key Technologies R&D Program of China (Nos. 2016YFA0201102 and 2017YFA0206200).

ORCID iD

Hao Wu https://orcid.org/0000-0001-8608-3035

References

- [1] Wolf S A, Awschalom D D, Buhrman R A, Daughton J M, von Molnar S, Roukes M L, Chtchelkanova A Y and Treger D M 2001 Spintronics: a spin-based electronics vision for the future *Science* 294 1488–95
- [2] Baibich M N, Broto J M, Fert A, Van Dau F N, Petroff F, Etienne P, Creuzet G, Friederich A and Chazelas J 1988 Giant magnetoresistance of (001)Fe/(001)Cr magnetic superlattices *Phys. Rev. Lett.* 61 2472–5
- [3] Binasch G, Grunberg P, Saurenbach F and Zinn W 1989 Enhanced magnetoresistance in layered magnetic structures with antiferromagnetic interlayer exchange *Phys. Rev.* B 39 4828–30
- [4] Parkin S, Xin J, Kaiser C, Panchula A, Roche K and Samant M 2003 Magnetically engineered spintronic sensors and memory *Proc. IEEE* 91 661–80
- [5] Julliere M 1975 Tunneling between ferromagnetic films Phys. Lett. A 54 225–6
- [6] Miyazaki T and Tezuka N 1995 Giant magnetic tunneling effect in Fe/Al₂O₃/Fe junction *J. Magn. Magn. Mater.* 139 L231–4
- [7] Moodera J S, Kinder L R, Wong T M and Meservey R 1995 Large magnetoresistance at room temperature in ferromagnetic thin film tunnel junctions *Phys. Rev. Lett.* 74 3273–6
- [8] Parkin S S P, Kaiser C, Panchula A, Rice P M, Hughes B, Samant M and Yang S-H 2004 Giant tunnelling magnetoresistance at room temperature with MgO (100) tunnel barriers *Nat. Mater.* 3 862

- [9] Yuasa S, Nagahama T, Fukushima A, Suzuki Y and Ando K 2004 Giant room-temperature magnetoresistance in single-crystal Fe/MgO/Fe magnetic tunnel junctions *Nat. Mater.* 3 868
- [10] Butler W H, Zhang X G, Schulthess T C and MacLaren J M 2001 Spin-dependent tunneling conductance of FelMgOlFe sandwiches *Phys. Rev.* B 63 054416
- [11] Berger L 1996 Emission of spin waves by a magnetic multilayer traversed by a current *Phys. Rev.* B **54** 9353–8
- [12] Slonczewski J C 1996 Current-driven excitation of magnetic multilayers J. Magn. Magn. Mater. 159 L1–L7
- [13] Martinez E, Emori S, Perez N, Torres L and Beach G S D 2014 Current-driven dynamics of Dzyaloshinskii domain walls in the presence of in-plane fields: full micromagnetic and one-dimensional analysis J. Appl. Phys. 115 213909
- [14] Zeinali B, Madsen J K, Raghavan P and Moradi F 2017 Ultra-fast SOT-MRAM cell with STT current for deterministic switching 2017 IEEE Int. Conf. on Computer Design (ICCD) pp 463–8
- [15] Perel M I D V I 1971 Possibility of orienting electron spins with current *JETP Lett.* **13** 467–9 (www.jetpletters.ru/ps/1587/article_24366.shtml)
- [16] Dyakonov V I P M I 1971 Current-induced spin orientation of electrons in semiconductors *Phys. Lett.* A 35 459
- [17] Hirsch J E 1999 Spin Hall effect *Phys. Rev. Lett.* **83** 1834–7
- [18] Zhang S F 2000 Spin Hall effect in the presence of spin diffusion *Phys. Rev. Lett.* **85** 393–6
- [19] Edelstein V M 1990 Spin polarization of conduction electrons induced by electric current in two-dimensional asymmetric electron systems *Solid State Commun*. 73 233–5
- [20] Dresselhaus G 1955 Spin-orbit coupling effects in zinc blende structures *Phys. Rev.* 100 580–6
- [21] Rashba R E and Bychkov Y A 1984 Properties of a 2D electron-gas with lifted spectral degeneracy *JETP Lett.* 30 78-81
- [22] Kim K-W, Seo S-M, Ryu J, Lee K-J and Lee H-W 2012 Magnetization dynamics induced by in-plane currents in ultrathin magnetic nanostructures with Rashba spin-orbit coupling *Phys. Rev.* B 85 180404
- [23] Wang X and Manchon A 2012 Diffusive spin dynamics in ferromagnetic thin films with a Rashba interaction *Phys. Rev. Lett.* 108 117201
- [24] Haney P M, Lee H-W, Lee K-J, Manchon A and Stiles M D 2013 Current induced torques and interfacial spin-orbit coupling: semiclassical modeling *Phys. Rev.* B 87 174411
- [25] Miron I M, Garello K, Gaudin G, Zermatten P J, Costache M V, Auffret S, Bandiera S, Rodmacq B, Schuhl A and Gambardella P 2011 Perpendicular switching of a single ferromagnetic layer induced by in-plane current injection *Nature* 476 189
- [26] Liu L, Pai C F, Li Y, Tseng H W, Ralph D C and Buhrman R A 2012 Spin-torque switching with the giant spin Hall effect of tantalum Science 336 555–8
- [27] Liu L, Pai C F, Ralph D C and Buhrman R A 2012 Magnetic oscillations driven by the spin Hall effect in 3-terminal magnetic tunnel junction devices *Phys. Rev. Lett.* 109 186602
- [28] Lee K-S, Lee S-W, Min B-C and Lee K-J 2013 Threshold current for switching of a perpendicular magnetic layer induced by spin Hall effect Appl. Phys. Lett. 102 112410
- [29] Yan S and Bazaliy Y B 2015 Phase diagram and optimal switching induced by spin Hall effect in a perpendicular magnetic layer *Phys. Rev.* B 91 214424
- [30] Peng S, Zhu D, Zhou J, Zhang B, Cao A, Wang M, Cai W, Cao K and Zhao W 2019 Modulation of heavy

- metal/ferromagnetic metal interface for high-performance spintronic devices *Adv. Electron. Mater.* **5** 1900134
- [31] Yu G et al 2014 Switching of perpendicular magnetization by spin-orbit torques in the absence of external magnetic fields Nat. Nanotechnol. 9 548-54
- [32] Yu G, Chang L-T, Akyol M, Upadhyaya P, He C, Li X, Wong K L, Amiri P K and Wang K L 2014 Current-driven perpendicular magnetization switching in Ta/CoFeB/[TaO_x or MgO/TaO_x] films with lateral structural asymmetry Appl. Phys. Lett. 105 102411
- [33] Chen T-Y, Chan H-I, Liao W-B and Pai C-F 2018 Current-induced spin-orbit torque and field-free switching in Mo-based magnetic heterostructures *Phys. Rev. Appl.* 10 044038
- [34] Razavi A, Wu H, Shao Q, Fang C, Dai B, Wong K, Han X, Yu G and Wang K L 2020 Deterministic spin-orbit torque switching by a light-metal insertion *Nano Lett*. 20 3703–9
- [35] Akyol M, Yu G, Alzate J G, Upadhyaya P, Li X, Wong K L, Ekicibil A, Amiri P K and Wang K L 2015 Current-induced spin-orbit torque switching of perpendicularly magnetized HflCoFeBlMgO and HflCoFeBlTaO_x structures Appl. Phys. Lett. 106 162409
- [36] Pai C-F, Mann M, Tan A J and Beach G S D 2016 Determination of spin torque efficiencies in heterostructures with perpendicular magnetic anisotropy *Phys. Rev.* B 93 144409
- [37] Razavi A, Wu H, Dai B, He H, Wu D, Wong K, Yu G and Wang K 2020 Spin–orbit torques in structures with asymmetric dusting layers Appl. Phys. Lett. 117 182403
- [38] Cui B et al 2019 Field-free spin-orbit torque switching of perpendicular magnetization by the Rashba interface ACS Appl. Mater. Interfaces 11 39369-75
- [39] Yu G et al 2016 Competing effect of spin-orbit torque terms on perpendicular magnetization switching in structures with multiple inversion asymmetries Sci. Rep. 6 23956
- [40] Torrejon J, Garcia-Sanchez F, Taniguchi T, Sinha J, Mitani S, Kim J-V and Hayashi M 2015 Current-driven asymmetric magnetization switching in perpendicularly magnetized CoFeB/MgO heterostructures *Phys. Rev.* B 91 214434
- [41] Chuang T C, Pai C F and Huang S Y 2019 Cr-induced perpendicular magnetic anisotropy and field-free spin-orbit-torque switching *Phys. Rev. Appl.* 11 061005
- [42] You L, Lee O, Bhowmik D, Labanowski D, Hong J, Bokor J and Salahuddin S 2015 Switching of perpendicularly polarized nanomagnets with spin orbit torque without an external magnetic field by engineering a tilted anisotropy *Proc. Natl Acad. Sci.* 112 10310
- [43] Dzyaloshinsky I 1958 A thermodynamic theory of 'weak' ferromagnetism of antiferromagnetics J. Phys. Chem. Solids 4 241–55
- [44] Moriya T 1960 Anisotropic superexchange interaction and weak ferromagnetism *Phys. Rev.* 120 91–98
- [45] Je S-G, Kim D-H, Yoo S-C, Min B-C, Lee K-J and Choe S-B 2013 Asymmetric magnetic domain-wall motion by the Dzyaloshinskii-Moriya interaction *Phys. Rev.* B 88 214401
- [46] Chen B, Lourembam J, Goolaup S and Lim S T 2019 Field-free spin-orbit torque switching of a perpendicular ferromagnet with Dzyaloshinskii-Moriya interaction Appl. Phys. Lett. 114 022401
- [47] Fert A, Reyren N and Cros V 2017 Magnetic skyrmions: advances in physics and potential applications *Nat. Rev. Mater.* 2 17031
- [48] Chen G et al 2013 Novel chiral magnetic domain wall structure in Fe/Ni/Cu(001) films Phys. Rev. Lett. 110 177204

[49] Wu H et al 2021 Chiral symmetry breaking for deterministic switching of perpendicular magnetization by spin–orbit torque Nano Lett. 21 515–21

- [50] MacNeill D, Stiehl G M, Guimaraes M H D, Buhrman R A, Park J and Ralph D C 2016 Control of spin–orbit torques through crystal symmetry in WTe2/ferromagnet bilayers Nat. Phys. 13 300–5
- [51] Han D-S et al 2019 Long-range chiral exchange interaction in synthetic antiferromagnets Nat. Mater. 18 703–8
- [52] Fernández-Pacheco A, Vedmedenko E, Ummelen F, Mansell R, Petit D and Cowburn R P 2019 Symmetry-breaking interlayer Dzyaloshinskii–Moriya interactions in synthetic antiferromagnets *Nat. Mater.* 18 679–84
- [53] Legrand W, Chauleau J-Y, Maccariello D, Reyren N, Collin S, Bouzehouane K, Jaouen N, Cros V and Fert A 2018 Hybrid chiral domain walls and skyrmions in magnetic multilayers Sci. Adv. 4 eaat0415
- [54] Li W et al 2019 Anatomy of Skyrmionic textures in magnetic multilayers Adv. Mater. 31 1807683
- [55] Zheng Z et al 2021 Field-free spin-orbit torque-induced switching of perpendicular magnetization in a ferrimagnetic layer with a vertical composition gradient Nat. Commun. 12 4555
- [56] Zhang K et al 2022 Efficient and controllable magnetization switching induced by intermixing-enhanced bulk spin-orbit torque in ferromagnetic multilayers Appl. Phys. Rev. 9 011407
- [57] Fukami S, Zhang C, DuttaGupta S, Kurenkov A and Ohno H 2016 Magnetization switching by spin-orbit torque in an antiferromagnet-ferromagnet bilayer system *Nat. Mater.* 15 535–41
- [58] Oh Y W et al 2016 Field-free switching of perpendicular magnetization through spin-orbit torque in antiferromagnet/ferromagnet/oxide structures Nat. Nanotechnol. 11 878–84
- [59] Li W, Peng S, Lu J, Wu H, Li X, Xiong D, Zhang Y, Zhang Y, Wang K L and Zhao W 2021 Experimental demonstration of voltage-gated spin-orbit torque switching in an antiferromagnet/ferromagnet structure *Phys. Rev.* B 103 094436
- [60] Peng S et al 2020 Exchange bias switching in an antiferromagnet/ferromagnet bilayer driven by spin–orbit torque Nat. Electron. 3 757–64
- [61] Peng S Z, Lu J Q, Li W X, Wang L Z, Zhang H, Li X, Wang K L and Zhao W S 2019 Field-free switching of perpendicular magnetization through voltage-gated spin-orbit torque *IEEE Int. Electron Devices Meeting* pp 28.26.21–24
- [62] van den Brink A, Vermijs G, Solignac A, Koo J, Kohlhepp J T, Swagten H J M and Koopmans B 2016 Field-free magnetization reversal by spin-Hall effect and exchange bias Nat. Commun. 7 10854
- [63] Razavi S A et al 2017 Joule heating effect on field-free magnetization switching by spin-orbit torque in exchange-biased systems Phys. Rev. Appl. 7 024023
- [64] Lau Y C, Betto D, Rode K, Coey J M and Stamenov P 2016 Spin-orbit torque switching without an external field using interlayer exchange coupling *Nat. Nanotechnol.* 11 758–62
- [65] Murray N, Liao W-B, Wang T-C, Chang L-J, Tsai L-Z, Tsai T-Y, Lee S-F and Pai C-F 2019 Field-free spin-orbit torque switching through domain wall motion *Phys. Rev.* B 100 104441
- [66] Garello K, Miron I M, Avci C O, Freimuth F, Mokrousov Y, Blügel S, Auffret S, Boulle O, Gaudin G and Gambardella P 2013 Symmetry and magnitude of spin-orbit torques in ferromagnetic heterostructures *Nat. Nanotechnol.* 8 587–93

- [67] Wang Z, Zhang L, Wang M, Wang Z, Zhu D, Zhang Y and Zhao W 2018 High-density NAND-like spin transfer torque memory with spin orbit torque erase operation *IEEE Electron Device Lett.* 39 343–6
- [68] Cai W et al 2021 Sub-ns field-free switching in perpendicular magnetic tunnel junctions by the interplay of spin transfer and orbit torques IEEE Electron Device Lett. 42 704–7
- [69] Kimata M et al 2019 Magnetic and magnetic inverse spin Hall effects in a non-collinear antiferromagnet Nature 565 627–30
- [70] Wang W et al 2019 Anomalous spin-orbit torques in magnetic single-layer films Nat. Nanotechnol. 14 819–24
- [71] Bose A, Lam D D, Bhuktare S, Dutta S, Singh H, Jibiki Y, Goto M, Miwa S and Tulapurkar A A 2018 Observation of anomalous spin torque generated by a ferromagnet *Phys. Rev. Appl.* 9 064026
- [72] Gibbons J D, MacNeill D, Buhrman R A and Ralph D C 2018 Reorientable spin direction for spin current produced by the anomalous Hall effect *Phys. Rev. Appl.* 9 064033
- [73] Hönemann A, Herschbach C, Fedorov D V, Gradhand M and Mertig I 2019 Spin and charge currents induced by the spin Hall and anomalous Hall effects upon crossing ferromagnetic/nonmagnetic interfaces *Phys. Rev.* B 99 024420
- [74] Luo Z, Zhang Q, Xu Y, Yang Y, Zhang X and Wu Y 2019 Spin-orbit torque in a single ferromagnetic layer induced by surface spin rotation *Phys. Rev. Appl.* 11 064021
- [75] Yu J et al 2019 Long spin coherence length and bulk-like spin-orbit torque in ferrimagnetic multilayers Nat. Mater. 18 29–34
- [76] Zhou J et al 2019 Large spin-orbit torque efficiency enhanced by magnetic structure of collinear antiferromagnet IrMn Sci. Adv. 5 eaau6696
- [77] Okuno T et al 2019 Spin-transfer torques for domain wall motion in antiferromagnetically coupled ferrimagnets Nat. Electron. 2 389–93
- [78] You Y et al 2021 Cluster magnetic octupole induced out-of-plane spin polarization in antiperovskite antiferromagnet Nat. Commun. 12 6524
- [79] Kondou K, Chen H, Tomita T, Ikhlas M, Higo T, MacDonald A H, Nakatsuji S and Otani Y 2021 Giant field-like torque by the out-of-plane magnetic spin Hall effect in a topological antiferromagnet *Nat. Commun.* 12 6491
- [80] Amin V P, Li J, Stiles M D and Haney P M 2019 Intrinsic spin currents in ferromagnets Phys. Rev. B 99 220405
- [81] Sun C, Deng J, Rafi-Ul-Islam S M, Liang G, Yang H and Jalil M B A 2019 Field-free switching of perpendicular magnetization through spin hall and anomalous hall effects in ferromagnet–heavy-metal–ferromagnet structures *Phys. Rev. Appl.* 12 034022
- [82] Seki T, Iihama S, Taniguchi T and Takanashi K 2019 Large spin anomalous Hall effect in L1₀–FePt: symmetry and magnetization switching *Phys. Rev.* B 100 144427
- [83] Li J-Y, Wang R-Q, Deng M-X and Yang M 2019 In-plane magnetization effect on current-induced spin-orbit torque in a ferromagnet/topological insulator bilayer with hexagonal warping *Phys. Rev.* B 99 155139
- [84] Sokolewicz R J, Ado I A, Katsnelson M I, Ostrovsky P M and Titov M 2019 Spin-torque resonance due to diffusive dynamics at the surface of a topological insulator *Phys.* Rev. B 99 214444
- [85] Ghosh S and Manchon A 2019 Nonequilibrium spin density and spin-orbit torque in a three-dimensional topological insulator/antiferromagnet heterostructure *Phys. Rev.* B 100 014412
- [86] Gweon H K, Lee K-J and Lim S H 2019 Influence of MgO sputtering power and post annealing on strength and angular dependence of spin-orbit torques in Pt/Co/MgO trilayers Phys. Rev. Appl. 11 014034

[87] Baek S H C, Amin V P, Oh Y W, Go G, Lee S J, Lee G H, Kim K-J, Stiles M D, Park B-G and Lee K-J 2018 Spin currents and spin-orbit torques in ferromagnetic trilayers *Nat. Mater.* 17 509–13

- [88] Kurebayashi D and Nagaosa N 2019 Theory of current-driven dynamics of spin textures on the surface of a topological insulator *Phys. Rev.* B 100 134407
- [89] Safranski C, Montoya E A and Krivorotov I N 2019 Spin–orbit torque driven by a planar Hall current *Nat. Nanotechnol.* 14 27–30
- [90] Humphries A M, Wang T, Edwards E R J, Allen S R, Shaw J M, Nembach H T, Xiao J Q, Silva T J and Fan X 2017 Observation of spin-orbit effects with spin rotation symmetry *Nat. Commun.* 8 911
- [91] Liu L et al 2021 Symmetry-dependent field-free switching of perpendicular magnetization Nat. Nanotechnol. 16 277–82
- [92] Liu L et al 2019 Current-induced magnetization switching in all-oxide heterostructures Nat. Nanotechnol. 14 939–44
- [93] Kong W J, Wan C H, Wang X, Tao B S, Huang L, Fang C, Guo C Y, Guang Y, Irfan M and Han X F 2019 Spin–orbit torque switching in a T-type magnetic configuration with current orthogonal to easy axes Nat. Commun. 10 233
- [94] Mishra R, Mahfouzi F, Kumar D, Cai K, Chen M, Qiu X, Kioussis N and Yang H 2019 Electric-field control of spin accumulation direction for spin-orbit torques *Nat. Commun.* 10 248
- [95] Wang X K K L, Upadhyaya P, Fan Y, Shao Q, Yu G and Amiri P K 2016 Electric-field control of spin-orbit interaction for low-power spintronics *Proc. IEEE* 104 1974–2008
- [96] Garello F Y K et al 2019 Manufacturable 300 mm platform solution for field-free switching SOT-MRAM Symp. on VLSI Circuits pp T194–5

- [97] Wu O G H et al 2018 Parasitic resistance reduction strategies for advanced CMOS FinFETs beyond 7 nm IEEE Int. Electron Devices Meeting (IEDM) pp 35.34.31–34
- [98] Wang Z, Li Z, Wang M, Wu B, Zhu D and Zhao W 2019 Field-free spin-orbit-torque switching of perpendicular magnetization aided by uniaxial shape anisotropy *Nanotechnology* 30 375202
- [99] Wang Z, Wu B, Li Z, Lin X, Yang J, Zhang Y and Zhao W 2018 Evaluation of ultrahigh-speed magnetic memories using field-free spin-orbit torque *IEEE Trans. Magn.* 54 1–5
- [100] Luo Y T Z, Dong Y, Lu C and Liu C W 2018 Field-free spin-orbit torque switching of perpendicular magnetic tunnel junction utilizing voltage-controlled magnetic anisotropy pulse width optimization Non-Volatile Memory Technology Symp. (NVMTS) pp 1–5
- [101] Honjo H et al 2019 First demonstration of field-free SOT-MRAM with 0.35 ns write speed and 70 thermal stability under 400 °C thermal tolerance by canted SOT structure and its advanced patterning/SOT channel technology IEEE Int. Electron Devices Meeting (IEDM) pp 28.25.21–24
- [102] Wang M et al 2018 Field-free switching of a perpendicular magnetic tunnel junction through the interplay of spin-orbit and spin-transfer torques Nat. Electron. 1 582–8
- [103] Fukami S, Anekawa T, Zhang C and Ohno H 2016 A spin-orbit torque switching scheme with collinear magnetic easy axis and current configuration *Nat. Nanotechnol.* 11 621–5
- [104] Alexander Makaro V S and Selberherr S 2018 Field-free fast reliable deterministic switching in perpendicular spin-orbit torque MRAM cells Int. Conf. on Simulation of Semiconductor Processes and Devices (SISPAD)
- [105] Cai K et al 2017 Electric field control of deterministic current-induced magnetization switching in a hybrid ferromagnetic/ferroelectric structure Nat. Mater. 16 712–6